The following Communications have been judged by at least two referees to be "very important papers" and will be published online at www.angewandte.org soon:

*J.-J. Li, T.-S. Mei, J.-Q. Yu**
Synthesis of Indolines and Tetrahydroisoquinolines from Arylethylamines by Palladium(II)-Catalyzed C–H Activation Reactions

*S. G. Srivatsan, N. J. Greco, Y. Tor**
Highly Emissive Fluorescent Nucleoside Signals the Activity of Toxic Ribosome-Inactivating Proteins

M. Mascal, E. B. Nikitin*
Direct, High-Yield Conversion of Cellulose into Biofuel

P. García-Álvarez, D. V. Graham, E. Hevia, A. R. Kennedy, J. Klett, R. E. Mulvey, C. T. O'Hara, S. Weatherstone*
Unmasking Representative Structures of TMP-Active Hauser and Turbo Hauser Bases

Books

Self Assembly — John A. Pelesko — *reviewed by J. R. Nitschke* ______ **6108**

Highlights

Protein Structures

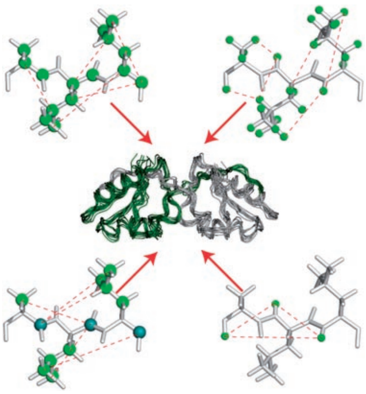

Protocols for determining high-resolution 3D structures of solid proteins are essential for structural studies of fibrils and membrane proteins. Advances in solid-state NMR spectroscopy have led to a multitude of approaches to access restraints and to calculate structures from highly ambiguous data sets. 3D structures at atomic resolution have been derived for several model proteins, as well as for the C-terminal portion of the Het-s prion protein.

A. Böckmann* ______ **6110 – 6113**

3D Protein Structures by Solid-State NMR Spectroscopy: Ready for High Resolution

Minireviews

Halogen Bonding

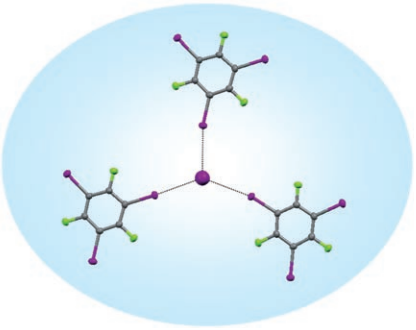

Building bridges: Halogen bonding is a noncovalent interaction where halogen atoms function as electrophilic species (see picture; gray C, green F, violet I). Halogen bonding has an impact on all fields where the control of recognition and self-organization plays a key role. The potential of the interaction is also shown by useful applications in the field of material science and in biological systems.

P. Metrangolo,* F. Meyer, T. Pilati, G. Resnati,* G. Terraneo ______ **6114 – 6127**

Halogen Bonding in Supramolecular Chemistry

Synthetic Networks

Z. Dadon, N. Wagner,
G. Ashkenasy* ______ **6128 – 6136**

The Road to Non-Enzymatic Molecular Networks

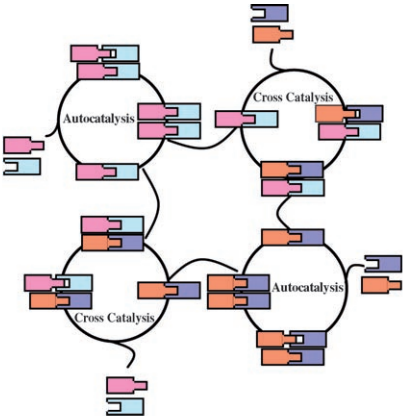

A systematic viewpoint: Recent progress in transforming minimal self-replicating systems into small networks of dynamically interacting molecules is reviewed. The authors suggest that such synthetic self-organized networks can provide useful models for studying the behavior of complex systems.

Reviews

Organocatalysis

P. Melchiorre,* M. Marigo,* A. Carlone,
G. Bartoli ______ **6138 – 6171**

Asymmetric Aminocatalysis—Gold Rush in Organic Chemistry

Gold! Gold! Gold from the American River! The seminal reports on asymmetric catalysis with secondary amines attracted waves of researchers to the “gold mine” of organocatalysis. Particular challenges, milestones, and future directions of asymmetric aminocatalysis are discussed in this Review.

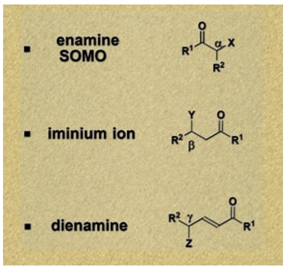

Communications

Microscopy

M. Heilemann,* S. van de Linde,
M. Schüttpelz, R. Kasper, B. Seefeldt,
A. Mukherjee, P. Tinnefeld,
M. Sauer* ______ **6172 – 6176**

Subdiffraction-Resolution Fluorescence Imaging with Conventional Fluorescent Probes

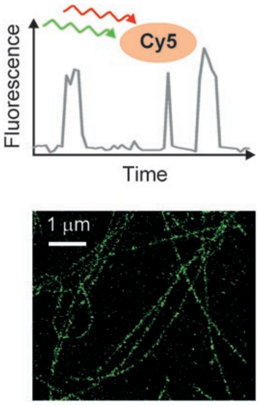

Eagle eyes: dSTORM uses conventional photoswitchable fluorescent dyes that can be reversibly cycled between a fluorescent and a dark state by irradiation with light of different wavelengths (see picture). This elegant approach can visualize cellular structures with a resolution of approximately 20 nm, far beyond the diffraction limit of light, without the need of an activator molecule.

For the USA and Canada:
ANGEWANDTE CHEMIE International Edition (ISSN 1433-7851) is published weekly by Wiley-VCH, PO Box 191161, 69451 Weinheim, Germany. Air freight and mailing in the USA by Publications Expediting Inc., 200 Meacham Ave., Elmont, NY 11003. Periodicals postage paid at Jamaica, NY 11431. US POSTMASTER: send address changes to *Angewandte Chemie*, Wiley-VCH, 111 River Street, Hoboken, NJ 07030. Annual subscription price for institutions: US$ 7225/6568 (valid for print and electronic / print or electronic delivery); for individuals who are personal members of a national chemical society prices are available on request. Postage and handling charges included. All prices are subject to local VAT/ sales tax.

Thin SiO_2 Films

J. Bachmann,* R. Zierold, Y. T. Chong, R. Hauert, C. Sturm, R. Schmidt-Grund, B. Rheinländer, M. Grundmann, U. Gösele, K. Nielsch* ____ **6177 – 6179**

A Practical, Self-Catalytic, Atomic Layer Deposition of Silicon Dioxide

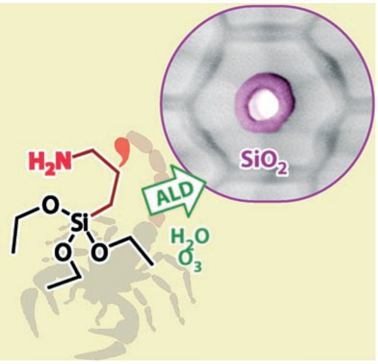

Molecular self-attack: According to mythology, a scorpion may sting itself to death; similarly, 3-aminopropyltriethoxysilane catalyzes its own hydrolysis in the atomic layer deposition (ALD) of SiO_2 thin films and nanostructures. Between 120 and 200 °C, the growth rate is constant at 0.06 nm per ALD cycle. The SiO_2 films are chemically and optically pure. SiO_2 nanotubes of aspect ratio 500 exhibit smooth walls of accurately controlled thickness.

Organocatalysis

C. E. Müller, L. Wanka, K. Jewell, P. R. Schreiner* ____ **6180 – 6183**

Enantioselective Kinetic Resolution of *trans*-Cycloalkane-1,2-diols

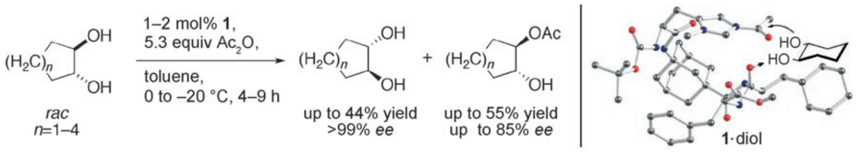

Finally! The title resolution is achieved with a nonnatural, partially rigid, lipophilic tetrapeptide at low catalyst loadings without additional base or cosolvents. The transition-state model (ball-and-stick model in the scheme; C gray, N blue, O red) emphasizes the interplay between hydrogen-bonding and hydrophobic interactions.

Protein Folding

F. Hillger, D. Hänni, D. Nettels, S. Geister, M. Grandin, M. Textor, B. Schuler* ____ **6184 – 6188**

Probing Protein–Chaperone Interactions with Single-Molecule Fluorescence Spectroscopy

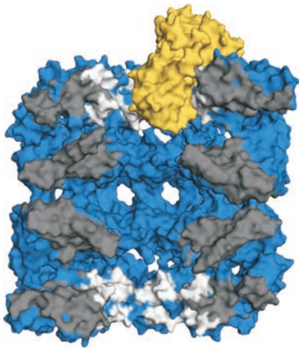

Molecular chaperones aid protein folding in the cell, but their effects on the conformation of the substrate protein have largely eluded experimental investigation. Single-molecule fluorescence spectroscopy was used to extract structural and dynamic information from a protein–chaperone complex (see figure; yellow: rhodanase, blue: GroEL). This approach will aid in a more physical understanding of the role of cellular factors in protein folding.

Natural Products Synthesis

M. Fleck, T. Bach* ____ **6189 – 6191**

Total Synthesis of the Tetracyclic Sesquiterpene (±)-Punctaporonin C

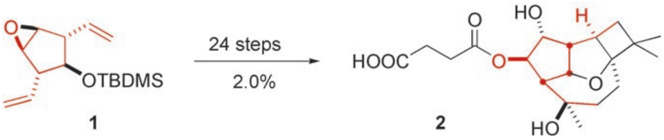

Tailor made for the target molecule **2**, the carbon skeleton of the epoxide **1** was integrated entirely into the natural product. A regioselective intramolecular [2+2] photocycloaddition and subsequent Wacker oxidation enabled the specific and successive incorporation of the two terminal double bonds of **1** into the unusual oxatetracyclo[6.3.2.0^{1,4}.0^{5,13}]tridecane skeleton of **2**, which was synthesized in 24 steps and 2.0% overall yield. TBDMS = *tert*-butyldimethylsilyl.

Incredibly reader-friendly!

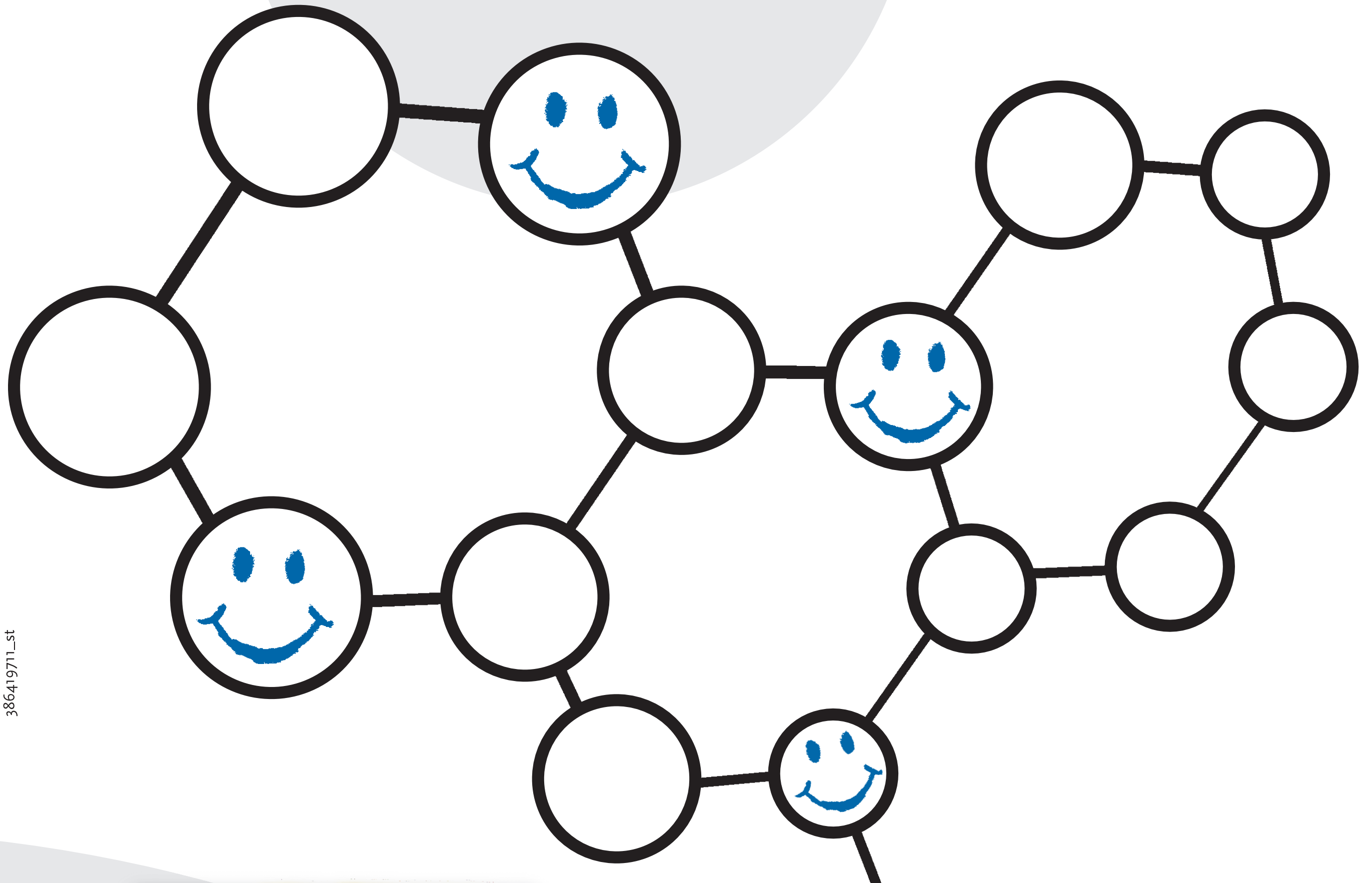

38641971_st

An aesthetically attractive cover picture that arouses curiosity, a well-presented and most informative graphical table of contents, and carefully selected articles that are professionally edited give *Angewandte Chemie* its distinctive character, which allows both easy browsing and further in-depth reading. Nearly 20 well-trained chemists, as well as eight further associates, work week in and week out to assemble reader-friendly issues and daily Early View articles online.

service@wiley-vch.de
www.angewandte.org

GDCh Gesellschaft Deutscher Chemiker

WILEY-VCH

Chelate Ligands

S. Roy, M. Sieger, B. Sarkar, B. Schwederski, F. Lissner, T. Schleid, J. Fiedler, W. Kaim* ________ 6192 – 6194

Establishing the Chelating α-Azocarbonyl Function in π-Acceptor Ligands

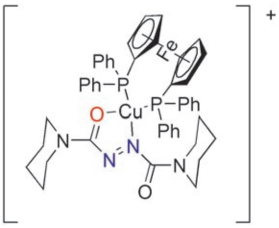

Strong acceptor, weak coordination: The heterodinuclear complex ion [LCu(dppf)]$^+$ (see formula) contains the as yet unrecognized strong π-acceptor system N=N–C=O, which is involved in a charge-transfer interaction with the copper center but is not reduced through full electron transfer. This situation is likely caused by steric hindrance and the donor function of the dialkylamino substituents on the C=O carbon atom.

Matter-Wave Interferometry

S. Gerlich, M. Gring, H. Ulbricht, K. Hornberger,* J. Tüxen, M. Mayor,* M. Arndt* ________ 6195 – 6198

Matter-Wave Metrology as a Complementary Tool for Mass Spectrometry

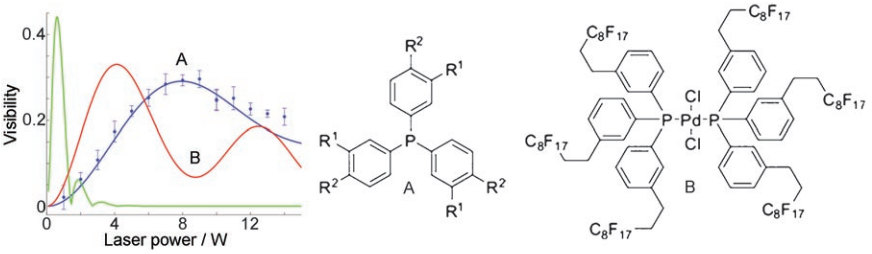

Quantum interferometry can serve as a useful complement to mass spectrometry. The interference visibility (see picture) reveals important information on molecular properties, such as mass and polarizability. The method is applicable to a wide range of molecules, and is particularly valuable for characterizing neutral molecular beams. In particular, fragmentation in the source can be distinguished from molecular dissociation in the detector.

Natural Products

K. Tiefenbacher,* J. Mulzer* 6199 – 6200

Short Formal Synthesis of (−)-Platencin

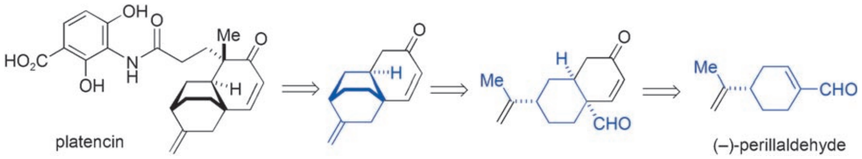

Short and sweet: A five-step, protecting-group-free formal synthesis of (−)-platencin from commercially available (−)-perillaldehyde (see retrosynthetic scheme) features a highly diastereoselective Diels–Alder reaction and a ring-closing metathesis as key steps.

Natural Products

S. Y. Yun, J.-C. Zheng, D. Lee* ________ 6201 – 6203

Concise Synthesis of the Tricyclic Core of Platencin

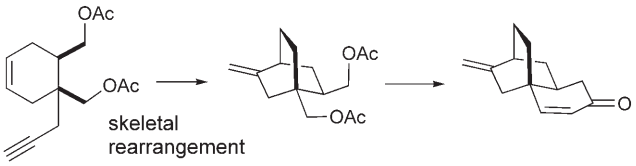

A radical change: Implementation of a radical-mediated rearrangement of the bicyclo[3.2.1]octyl moiety to the bicyclo[2.2.2]octane structure has enabled a concise synthesis of the tricyclic core of platencin, a newly discovered antibiotic. An intramolecular aldol and a ring-closing metathesis reaction were subsequently used to complete the synthesis of the tricycle (see scheme).

Contents

Higher Fullerenes

I. E. Kareev,* I. V. Kuvychko,
N. B. Shustova, S. F. Lebedkin,
V. P. Bubnov, O. P. Anderson, A. A. Popov,
O. V. Boltalina,*
S. H. Strauss* ______ **6204 – 6207**

C_1-(C_{84}-C_2(11))(CF_3)$_{12}$: Trifluoromethylation Yields Structural Proof of a Minor C_{84} Cage and Reveals a Principle of Higher Fullerene Reactivity

Ribbon pattern: An isomer of $C_{84}(CF_3)_{12}$ fullerene with the C_{84}-C_2(11) cage (see molecular structure determined by X-ray crystallography) demonstrates a new principle of hollow higher fullerene reactivity: For 1,4-additions of bulky groups that produce ribbons or loops of edge-sharing *p*-C_6X_2 hexagons, the "most reactive" double bonds remain intact.

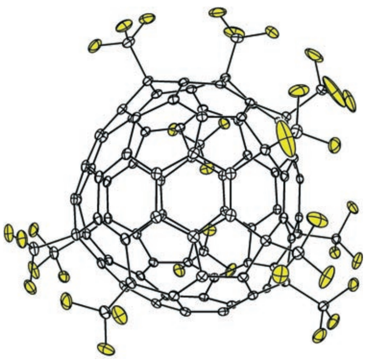

Polymetalation

V. L. Blair, L. M. Carrella, W. Clegg,
B. Conway, R. W. Harrington, L. M. Hogg,
J. Klett, R. E. Mulvey,* E. Rentschler,
L. Russo ______ **6208 – 6211**

Tuning the Basicity of Synergic Bimetallic Reagents: Switching the Regioselectivity of the Direct Dimetalation of Toluene from 2,5- to 3,5-Positions

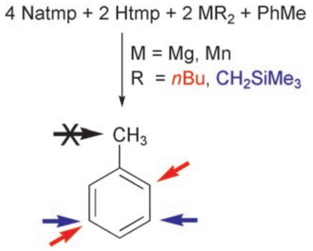

***Meta–meta* metalation**: Remarkably, toluene can be directly dimanganated or dimagnesiated at the 3,5-positions using bimetallic bases with active Me_3SiCH_2 ligands (see scheme, blue). In contrast, *n*-butyl ligands lead to 2,5-metalation (red). tmp = 2,2,6,6-tetramethylpiperidide.

Boron–Nitrogen Compounds

A. Staubitz, A. Presa Soto,
I. Manners* ______ **6212 – 6215**

Iridium-Catalyzed Dehydrocoupling of Primary Amine–Borane Adducts: A Route to High Molecular Weight Polyaminoboranes, Boron–Nitrogen Analogues of Polyolefins

The B all and N all: Soluble, linear, high molecular weight polyaminoborane homopolymers and copolymers have been synthesized by iridium-catalyzed dehydrocoupling of readily available amine–borane adducts $RNH_2{\cdot}BH_3$ (R = H, Me, *n*Bu).

Conformational Analysis

M. E. Sanz, S. Blanco, J. C. López,
J. L. Alonso* ______ **6216 – 6220**

Rotational Probes of Six Conformers of Neutral Cysteine

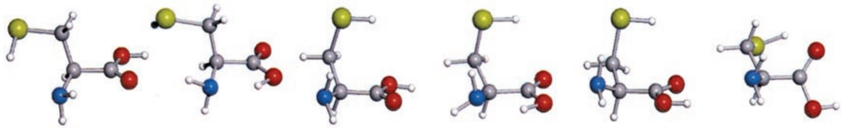

Six of one: Vaporization of solid cysteine by laser ablation followed by the generation of a supersonic jet in a vacuum chamber has enabled six low-energy conformers of this amino acid to be characterized by using Fourier transform microwave spectroscopy (see picture). The information provided by this technique is directly comparable with that predicted from in vacuo ab initio computations.

Ex situ synthesis is the key: Palladium nanoparticles having a narrow size distribution around 3.6 nm have been synthesized in a liquid phase and then loaded onto a carbon support with an overall efficiency of 85 %. The resulting nanoparticles, which retained their size and morphology, were exceptionally active and selective as a catalyst for the direct formation of H_2O_2 from H_2 and O_2 in ethanol.

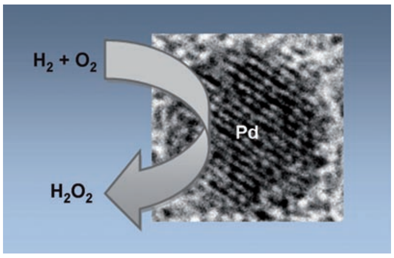

Nanoparticle catalysis

Q. Liu, J. C. Bauer, R. E. Schaak,
J. H. Lunsford* ———— **6221 – 6224**

Supported Palladium Nanoparticles: An Efficient Catalyst for the Direct Formation of H_2O_2 from H_2 and O_2

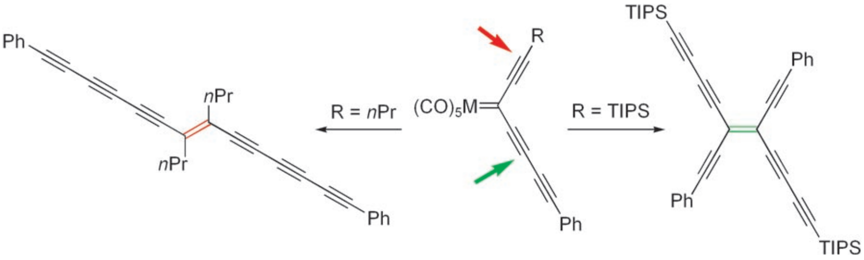

Heads or tails? Chemo-, regio-, and stereoselective access to cross- and linear conjugated poly-yne scaffolds from alkynyl-derived group six metal carbenes is reported. The metal carbenes shown ($M = Cr, W$; TIPS = triisopropylsilyl) readily undergo low-temperature, tail-to-tail dimerization in the presence of potassium *tert*-butoxide by reaction at either of the C_β atoms to provide *E*-polyalkynylethenes.

Synthetic Methods

J. Barluenga,* D. de Sáa, A. Gómez,
A. Ballesteros, J. Santamaría,
A. de Prado, M. Tomás,
A. L. Suárez-Sobrino ———— **6225 – 6228**

Metal Carbene Dimerization: Versatile Approach to Polyalkynylethenes

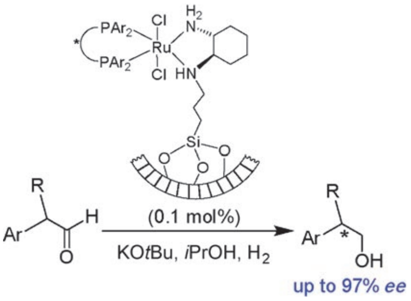

Chiral Ruthenium–diphosphine–diamine complexes with a siloxy pendant are grafted onto mesoporous silica nanospheres. The resulting supported ruthenium catalysts are highly active for the asymmetric hydrogenation of aromatic ketones to afford chiral secondary alcohols and racemic aryl aldehydes to give chiral primary alcohols (see scheme). This immobilization strategy should be amenable to the design of similar heterogeneous catalysts.

Supported Catalysts

D. J. Mihalcik, W. Lin* ———— **6229 – 6232**

Mesoporous Silica Nanosphere Supported Ruthenium Catalysts for Asymmetric Hydrogenation

Gaining control: An attractive electrostatic force stabilizes the conformation of an intermediate (see scheme; n = nonbonded electron), thus controlling the leaving group configuration to give superior diastereoselectivity in an asymmetric ring expansion.

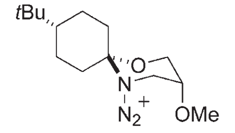

attractive cation–n interaction

Asymmetric Ring Expansion

T. Ribelin, C. E. Katz, D. G. English,
S. Smith, A. K. Manukyan, V. W. Day,
B. Neuenswander, J. L. Poutsma,*
J. Aubé* ———— **6233 – 6235**

Highly Stereoselective Ring Expansion Reactions Mediated by Attractive Cation–n Interactions

Contents

Nitrogen-Rich Compounds

Y.-H. Joo, B. Twamley, S. Garg,
J. M. Shreeve* ______ **6236 – 6239**

Energetic Nitrogen-Rich Derivatives of 1,5-Diaminotetrazole

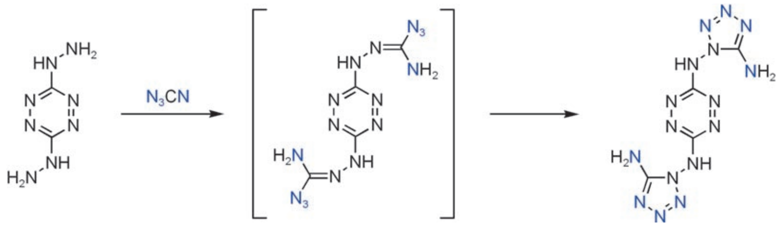

High-energy-density materials can be obtained by reaction of monosubstituted hydrazines with cyanogen azide to generate 1,5-diaminotetrazole derivatives. Azidohydrazones are postulated as intermediates in this reaction (see scheme).

Molecular Logic

M. Amelia, M. Baroncini,
A. Credi* ______ **6240 – 6243**

A Simple Unimolecular Multiplexer/Demultiplexer

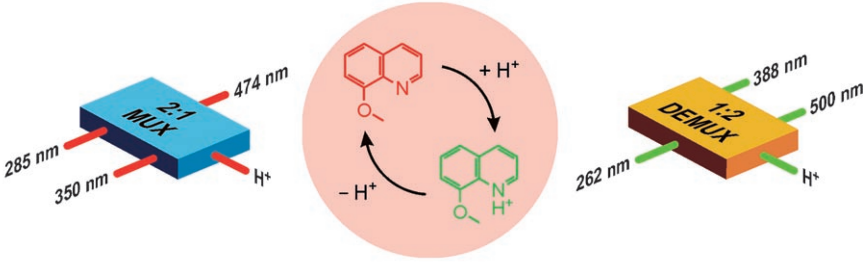

Simple but effective! 8-Methoxyquinoline, an unsophisticated fluorophore, displays both 2:1 multiplexer and 1:2 demultiplexer digital functions (see picture). Protonation of the fluorophore results in completely different optical spectral profiles and multiplexing/demultiplexing behavior is obtained by exploiting the proton-driven reversible modulation of two complementary absorption and fluorescence signals.

Heterocycle Synthesis

K. Takahashi, M. Midori, K. Kawano,
J. Ishihara, S. Hatakeyama* **6244 – 6246**

Entry to Heterocycles Based on Indium-Catalyzed Conia-Ene Reactions: Asymmetric Synthesis of (−)-Salinosporamide A

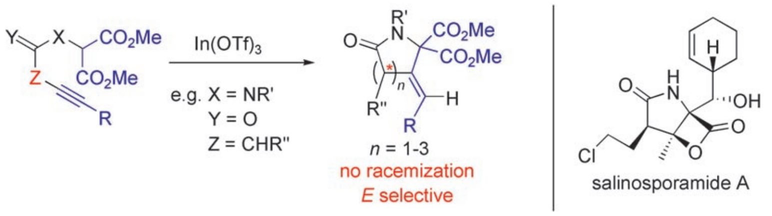

Conica can: The In(OTf)$_3$-catalyzed cyclization of nitrogen- and oxygen-tethered acetylenic malonic esters gives five- to seven-membered heterocycles in moderate to excellent yields (see scheme; Tf = trifluoromethanesulfonyl). The asymmetric synthesis of (−)-salinosporamide A illustrates the synthetic utility of the method.

Protein Structures

C. Uetrecht, C. Versluis, N. R. Watts,
P. T. Wingfield, A. C. Steven,
A. J. R. Heck* ______ **6247 – 6251**

Stability and Shape of Hepatitis B Virus Capsids In Vacuo

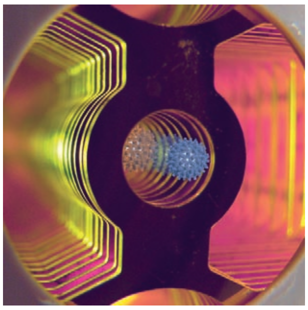

Viruses at a glance: Ion mobility mass spectrometry allows the identification and differentiation of states in a viral assembly not only by mass but also by conformation. This approach has been used to obtain a biophysical characterization of the hepatitis B virus capsids, and has shown that of its two distinct icosahedral geometries, the spherical capsid structure is preserved in vacuo (see picture).

Actinoid Chemistry

A.-G. D. Nelson, T. H. Bray,
T. E. Albrecht-Schmitt* ______ **6252 – 6254**

Capitalizing on Differing Coordination Environments and Redox Potentials to Prepare an Ordered Heterobimetallic U^{VI}/Np^{IV} Diphosphonate

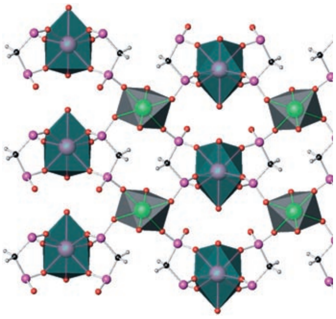

Order out of chaos: The reduction of Np^{VI} to Np^{IV} readily occurs under mild hydrothermal conditions in the presence of phosphonates, sharply contrasting with U^{VI}, which maintains its oxidation state under identical conditions. By coupling the differing redox potentials of U^{VI} and Np^{VI} with the vastly different coordination chemistry of U^{VI} and Np^{IV}, the first example of an ordered U^{VI}/Np^{IV} phosphonate is prepared (see structure: U green, Np purple (large), O red, P purple (small)).

Supramolecular Chemistry

N. Nishimura,
K. Kobayashi* ______ **6255 – 6258**

Self-Assembly of a Cavitand-Based Capsule by Dynamic Boronic Ester Formation

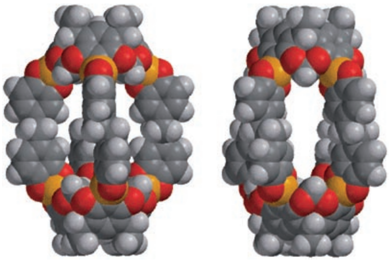

Be my guest: Two molecules of a cavitand tetraboronic acid and four molecules of a bis(catechol) linker quantitatively assemble into a capsule (see picture for two views), with highly selective guest-recognition, by dynamic boronic ester formation. The on/off control of capsule formation with guest encapsulation is achieved by removal/addition of methanol.

Imaging Probe

J.-s. Choi, J. C. Park, H. Nah, S. Woo, J. Oh, K. M. Kim, G. J. Cheon, Y. Chang, J. Yoo,* J. Cheon* ______ **6259 – 6262**

A Hybrid Nanoparticle Probe for Dual-Modality Positron Emission Tomography and Magnetic Resonance Imaging

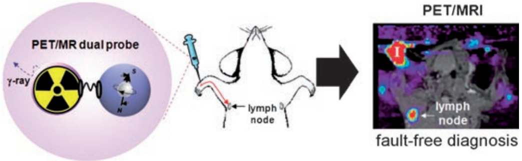

Creating a good image: A probe for combined positron emission tomography (PET) and magnetic resonance imaging (MRI) has high colloidal stability and demonstrates facile conjugation ability. Sentinel lymph nodes are clearly identified in the fusion image (see picture; I: injection site) because of the complementary nature of the techniques, which makes accurate anatomical information and fault-free diagnosis possible.

Bionanoreactors

B. Le Droumaguet,
K. Velonia* ______ **6263 – 6266**

In Situ ATRP-Mediated Hierarchical Formation of Giant Amphiphile Bionanoreactors

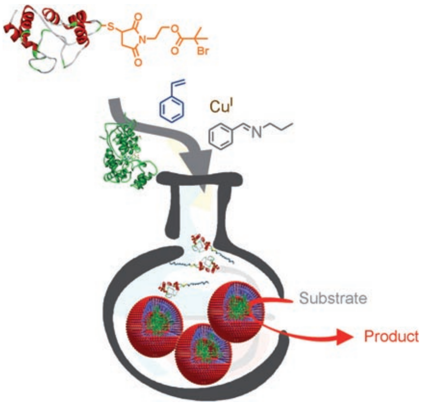

Functional giants: Amphiphilic bioconjugates can be synthesized in situ by grafting polystyrene from a protein (see scheme). The resulting giant amphiphiles display low polydispersities and the characteristic aggregation properties of amphiphilic biomacromolecules. A second, catalytically active guest protein can also be included within the superstructures.

Contents

Electroactive Monolayers

E. W. L. Chan, S. Park,
M. N. Yousaf* ______________ **6267 – 6271**

An Electroactive Catalytic Dynamic Substrate that Immobilizes and Releases Patterned Ligands, Proteins, and Cells

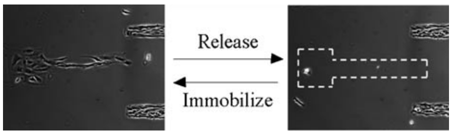

Dynamic release: A quinone-terminated self-assembled monolayer captures and releases ligands and cells in situ through a pH-dependent electrochemical potential. The surface is catalytic for multiple rounds of immobilization/release. When combined with a photochemical approach, peptide ligands that mediate cell attachment are captured and released on defined gradient patterns (see picture).

Intracluster Proton Transfer

I. Wolf, A. Shapira, R. Giniger, Y. Miller,
R. B. Gerber,
O. Cheshnovsky* ____________ **6272 – 6274**

Critical Size for Intracluster Proton Transfer from Water to an Anion

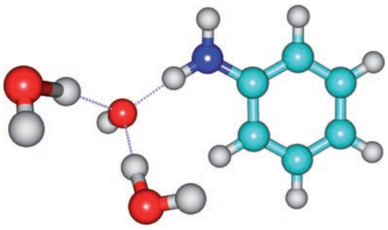

Bigger is better: Proton transfer in the electronic ground state for $(C_6H_5NH^-)\cdot(H_2O)_n$ has been investigated by photoelectron spectroscopy. At a critical size of $n=3$, one proton of a water molecule is captured by the deprotonated aniline to form solvated OH^- (see picture). These experimental observations are supported by ab initio calculations that establish the greater stability of the solvated OH^- anion for $n \geq 3$.

Molecular Interactions

J. L. Cook, C. A. Hunter,* C. M. R. Low,
A. Perez-Velasco,
J. G. Vinter ______________ **6275 – 6277**

Preferential Solvation and Hydrogen Bonding in Mixed Solvents

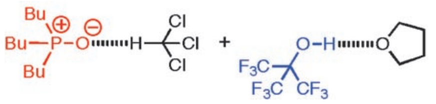

Oak trees from acorns: A small amount (<1%) of a cosolvent can change the stability of the H-bonded complex on the right-hand side of the equation by an order of magnitude. Mixtures of chloroform and THF were found to be more polar than either of the pure solvents by using this complex as a molecular-recognition probe of solvation. A quantitative interpretation based on preferential solvation accounts for the properties of solvent mixtures.

Synthetic Methods

G. Deng, L. Zhao, C.-J. Li* _ **6278 – 6282**

Ruthenium-Catalyzed Oxidative Cross-Coupling of Chelating Arenes and Cycloalkanes

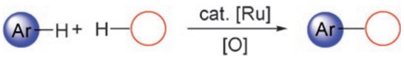

Alkane and arene join together: Various arenes were coupled directly with simple cycloalkanes. The reaction was catalyzed by ruthenium under oxidative conditions to give substituted cycloalkylarenes regioselectively (see scheme).

Fullerenes

K. S. Simeonov, K. Y. Amsharov, E. Krokos,
M. Jansen* _______________ **6283 – 6285**

An Epilogue on the C_{78}-Fullerene Family: The Discovery and Characterization of an Elusive Isomer

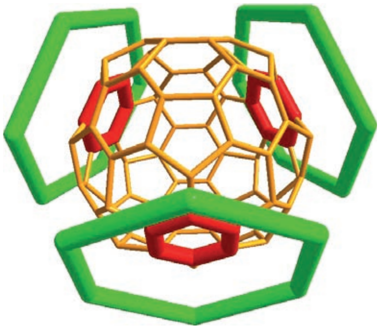

Missing relative found: The last representative of the first multi membered fullerene family, $C_{78}(4)$, has been synthesized and isolated. Its connectivity pattern was confirmed by a single-crystal X-ray analysis of its chlorinated derivative $C_{78}(4)Cl_{18}$ (see picture). The crystal structure also reveals the presence of unusual, short intermolecular chlorine contacts.

Liquid crystals shining bright. A highly efficient platinum(II) luminophore is rendered liquid crystalline using a simple and flexible synthetic approach. Ordering in the liquid-crystalline state allows monomer emission when the characteristic for the material is exciplex-like emission. More than that, emission characteristics are subject to tribological control, with the initial state re-obtained by thermal cycling.

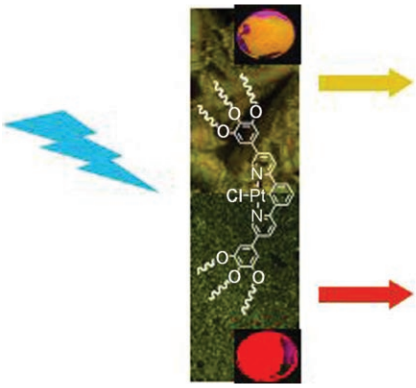

Metallomesogens

V. N. Kozhevnikov,* B. Donnio,
D. W. Bruce* ———— **6286–6289**

Phosphorescent, Terdentate, Liquid-Crystalline Complexes of Platinum(II): Stimulus-Dependent Emission

A model solution to hydrogen storage? The recently introduced hydrogen storage material [{Ca(NH$_2$BH$_3$)$_2$}$_n$] has been investigated on a molecular level. A hydrocarbon-soluble calcium amidoborane complex eliminates H$_2$ spontaneously at the very low temperature of 20–40 °C (see scheme). The decomposition product shows a dimeric species with a bridging [HN−BH−NH−BH$_3$]$^{2-}$ ion that is isolobal to the allylic dianion [HC−CH−CH−CH$_3$]$^{2-}$.

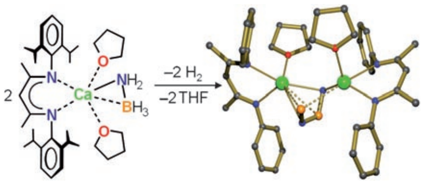

Hydrogen Storage

J. Spielmann, G. Jansen, H. Bandmann,
S. Harder* ———— **6290–6295**

Calcium Amidoborane Hydrogen Storage Materials: Crystal Structures of Decomposition Products

Supporting information is available on www.angewandte.org (see article for access details).

A video clip is available as Supporting Information on www.angewandte.org (see article for access details).

Service

Spotlights Angewandte's Sister Journals ———— ***6106–6107***

Keywords ———— ***6296***

Authors ———— ***6297***

Vacancies ———— ***6105***

Preview ———— ***6299***